Fuel 312 (2022) 122709

Contents lists available at ScienceDirect

Fuel

journal homepage: www.elsevier.com/locate/fuel

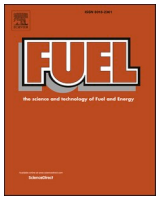

Full Length Article

Towards fuel composition and properties from Two-dimensional gas chromatography with flame ionization and vacuum ultraviolet spectroscopy

Joshua Heyne *, David Bell, John Feldhausen, Zhibin Yang, Randall Boehm

University of Dayton, Dayton, OH, USA

ARTICLE INFO

Keywords:
Property modeling
Jet fuel
Sustainable aviation fuel
GCxGC
VUV

ABSTRACT

Already low volume (<1mL) test methods facilitate the development of sustainable aviation fuel platforms and higher fidelity computational methods. Here a novel technique with two-dimensional gas chromatography (GCxGC) and Vacuum Ultraviolet (VUV) identification is used to characterize fuel composition and determine properties compared to previous work. Ten properties are predicted, including the temperature dependence of density, viscosity, thermal conductivity, and heat capacity. Property predictions incorporate uncertainty quantification (UQ) from analyte quantification (UQ1), root property uncertainty (UQ2), and the uncertainty associated with isomeric variance (UQ3), when an analyte is not identified via VUV. Comparisons to a previous method illustrate the ability of VUV identification to increase the fidelity of property predictions and decrease uncertainties. This method is applied to a surrogate intended to mimic the first-order properties and composition of a representative Jet A/A-1. In addition to nominal and temperature-dependent properties, the derived cetane number (DCN) of the surrogate is calculated for the distillation fraction evolved. The DCN there is shown to vary across the fraction of fuel distilled. Collectively, this method documents a process to prescreen novel sustainable aviation fuel candidates, facilitate the development of chemical process models, and automate property determinations for computational fluid dynamics.

1. Introduction

Advances in analytical chemistry and computational capabilities facilitate sustainable, clean, and efficient transportation technologies. These methods have enabled the development of feedstock-conversion ideas to processes that produce requisite testing volumes in less than a year [1]. In turbine aviation fuels, several studies have been published on predicting fit-for-purpose properties aimed at evaluating the potential of sustainable aviation fuel (SAF) candidates to advance from low technology readiness levels and de-risk low carbon technologies [2–6]. In parallel, ASTM standards and research tools have been developed to support computational fluid dynamics and chemical kinetic model development [3,7–9]. Two predictive methodologies have been the focus of intense recent advancements. Specifically, (1) bottom-up models build bulk or collective fluid properties from composition data derived from multidimensional gas chromatography with fundamental [10] or semi-empirical models [3]. While the other method, (2) top-down models, interpolated from trained data to predict fluid properties with the 'goodness of fit' reported. Both bottom-up and top-down models collectively leverage the relationships between chemical structure, spectroscopic data, two-dimensional gas chromatography hydrocarbon type determinations, and other material properties [4–6,11–15]. Collectively, these test methods are maturing low carbon technologies quickly (hours) with the lowest volume requirements (<1mL).

There are practical uncertainty quantification implications when taking either approach. Bottom-up models can define 'known-unknowns' as a function of the potential of isomeric structures and other physical parameters and are limited in accuracy by root data and models

Abbreviations: ρ, density; *n*, number of carbons in an analyte; *N*, number of analytes detected; σ, surface tension or standard deviation; λ, wavelength; t_1, first time GCxGC dimension; t_2, second time GCxGC dimension; *Y*, mass fraction; *Z*, generic property of interest; ASTM, ASTM International; CI, confidence interval; DCN, derived cetane number; FID, flame ionization detector; GC, one-dimensional or generic gas chromatography; GCxGC, two-dimensional gas chromatography; LHV, lower heating value or heat of combustion; MS, mass spectrometry; m%, mass percent; SAF, sustainable aviation fuel; VUV, vacuum ultraviolet light detector.

* Corresponding author.
E-mail address: jheyne1@udayton.edu (J. Heyne).

https://doi.org/10.1016/j.fuel.2021.122709
Received 27 September 2021; Received in revised form 15 November 2021; Accepted 22 November 2021
Available online 15 December 2021

used to make predictions. This method of uncertainty quantification means the quantification of uncertainty is straightforward but tedious, and the predictive fidelity is not anchored to the measurement it is aiming to predict. In the case of previous work, the lower heating value (LHV) of a fuel can be determined accurately as (a) the root data is accurately defined, (b) there is a significant amount of data on the influence of isomers, and (c) the model for determining the LHV of a mixture is fundamentally defined [10]. However, in the case of viscosity, there are issues within this approach (a) to (c); (a) there is less accurately defined root data, (b) there is less data on the influence of isomers, and (c) there is a semi-empirical model applied due to the fundamental model's computational expense. For top-down approaches, the problems are inverted versus bottom-up approaches. Top-down models risk extrapolating to a non-physical result. The extrapolation makes the quantifying of uncertainty experimentally tedious, and the accuracy of the predictions is rooted in the training dataset. Since they are not tuned to target data, bottom-up approaches do not need training data, and modeling uncertainties are sourced in the independent data used to generate predictions. Top-down approaches need training data, and depending on the complexity of the model, many times more data are needed for uncertainty quantification.

Additionally, for top-down methods, thermochemical properties and chemical kinetic models have been developed from an infrared measurement of quiescent and reacting systems and nuclear magnetic resonance [11–13,15–17]. These models are then coupled to statistical packages to approximate kinetics or predict relevant physical properties. To date, one such model [12] has demonstrated correlation (adjusted $R^2 > 0.9$) between FTIR data and several fit-for-purpose properties, including; surface tension, lower heating value, derived cetane number, bubble point, and final boiling point within a training data set that contains 15–32 samples. Compared to other engineering methods, these methods are still relatively new, and the boundaries of their applicability are yet to be defined. One apparent limitation of these methods is the lack of compositional and other variances across the distillation range; two examples of these limitations are mentioned here. Gradients that are important across the distillation curve are not yet captured with mid-infrared or nuclear magnetic resonance without coupling to a gas chromatogram or fractional distillation and multiple samples evaluated. Specifically, events like preferential vaporization [18] are likely unpredictable with mid-infrared spectroscopy and nuclear magnetic resonance unless coupled with a separation method. Additionally, the fractionation and identification of specific chemical compositions by hydrocarbon type and carbon number are unavailable. This data informs fuel producers about feedstock and processing methods' impact on composition.

Two-dimensional gas chromatography has shown the ability to consistently separate hydrocarbons into bins [3,19], with demonstrated 3-dimensional chromatography showing even more promise to distinguish analytes [20]. In these methods, analytes are separated, to first order, by their volatility and polarity. The analytes are modulated between columns to maintain separations from the previous column, with each modulation potentially having several analytes that are then, ideally, separated on subsequent column(s). Analytes are then sent to a detector, such as a flame ionization detector (FID), a mass spectrometer (MS), or an optical spectral analyzer. FIDs, known for consistency and broad detection ranges, are typically used for quantification, but they provide no information about specific isomers that may coelute through each column of the gas chromatography machine. As a result, there is significant uncertainty associated with fuel properties determinations built from GCxGC-FID data and a large (1,226 molecule) reference database [3]. The wide range of properties among molecules in the same hydrocarbon class is at the root of this variance. For example, the variance for freeze point across 17 *iso*-alkanes with 8 carbons is >200 °C. Meaning, the uncertainty of freeze points determinations without specific isomeric information will remain significant. In total, multidimensional gas chromatography with FID quantification is excellent for precise (better than 0.1 m%) and accurate (~0.2 m% for a given carbon number and hydrocarbon type) quantifications and characterization of fuel compositions by hydrocarbon type and carbon number [21].

Once analytes are separated, mass spectrometers (MS) or optical spectral analyzers are used in tandem with FID to identify analytes. A review of all the strengths and weaknesses of MS detectors is beyond the scope of this paper. However, of note here, MS detectors are excellent in the delineation of major hydrocarbon structure classifications, i.e., aromatics from saturates. However, MS detectors are not known to provide data sufficient to reliably identify specific isomers, such as o-, m-, or p-xylene or the stereoisomers of decalin. Specifically, the ability to distinguish between branching has not been demonstrated for GCxGC methods (Vozka and Gozdem [14]). Distinguishing between branching was referred there as a next step for GCxGC methods a series of papers on property predictions, including GCxGC-MS methods.

Alternatively, gas chromatography can be coupled with absorption spectroscopy to speciate analytes. For example, Wang recently applied GCxGC-VUV to analyze diesel fuel [22], and Anthony et al. [23] recently demonstrated enhanced isomer selectivity of GC-VUV-MS relative to GC–MS. Lelevic et al. [24] have recently published a review article on the topic. Additionally, a recent VUV study has illustrated the ability to deconvolute coeluting peaks [25] quantitatively. These VUV studies have illuminated the ability to distinguish between stereo and structural isomers, but they have not been leveraged to predict fit-for-purpose properties. Fig. 1 illustrates some examples of the capacity for VUV spectra to distinguish between spectra for trimethyl benzenes (TMB) and decalins. In summary, the benefit of coupling multidimensional gas chromatograms to spectroscopy is that it offers the potential to identify stereo and structural isomers, which contribute significantly to the aviation fuel property variance.

With multidimensional gas chromatography providing analyte identification and quantification, many properties can be determined from that data with a library of constituent properties and fundamental or semi-empirical blending rules for each property of interest. Moreover, uncertainty quantification is well defined for this approach; for example, see Yang et al. [3] and Boehm et al. [10]. Conversely, approaches that train diagnostic data directly to known properties (regardless of statistical method) are top-down, and comprehensive uncertainty quantification that incorporates uncertainties imparted from all independent data and models is experimentally difficult. Predictive error is not comprehensive uncertainty; see discussion by Heyne et al. [2]. The quantification of uncertainty is beyond the statistical variance of a numerical method. Species size (~molecular weight), structural features, and chemical bonds (~polarity) are all critical in prescreening alternative fuels. Assumptions cannot be made about the population distribution of molecular sizes or types without conveying the consequential uncertainty introduced by these assumptions. Two sustainable aviation fuel blend components, defined by ASTM D7566 specifications, are composed of very selective and specific isomers (Annexes A3 and A5 [*iso*-butanol] [26]. If a predictive method is not tempered with comprehensive uncertainty quantification, recommendations could be unfounded, and resources squandered at a critical moment in transportation decarbonization. There is a growing list of ASTM methods that are useful for conventional fuels but ill-suited alternative fuels such as ASTM D3338 (LHV) [10] and ASTM D4737 (cetane index).

Robust separations with calibrated multidimensional gas chromatograms, absorption spectroscopy, and large hydrocarbon databases offer the potential to quantify and identify analytes directly and predict many nuanced properties of hydrocarbon fuels. Here we report the first case study of property predictions for modeling and prescreening SAFs using two-dimensional gas chromatography, vacuum ultraviolet spectroscopy for identification, and flame ionization detection for quantification with uncertainty quantification. Identification of analytes is done in the absence of any retention time information from the GCxGC; identification is not calibrated to the chromatogram. Separation here is only meant to separate analytes for VUV spectra matching. Predictions

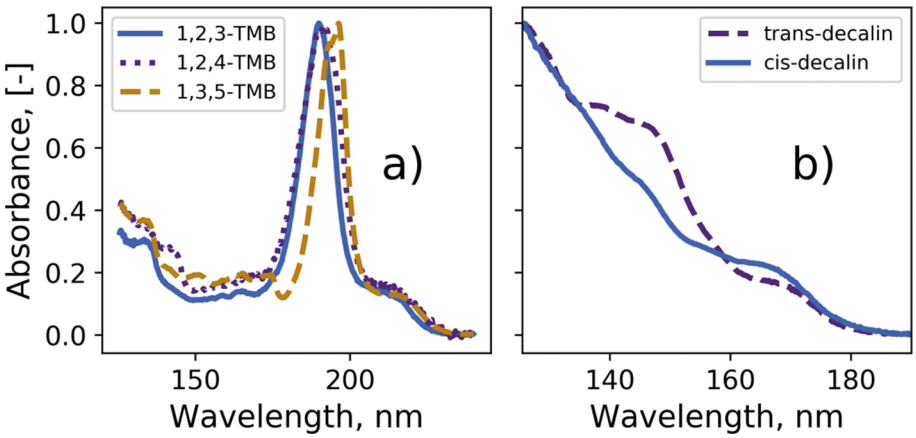

Fig. 1. Normalized sample reference spectra for trimethyl benzene (TMB) structural isomers a) and decalin stereoisomers b). The variance between TMBs and decalins is easily distinguished and repeatable with a VUV detector.

of 10 properties, including confidence intervals, based on the method of Yang et al. [3] are compared to the new method detailed in this paper for one aviation turbine surrogate composition. For reference, several of these comparisons also include a nominal value corresponding to a direct measurement derived from an applicable ASTM standard experimental method.

2. Experimental and computational methods

Two deterministic approaches were used to derive fit-for-purpose fuel properties that impact combustor/engine operability in jet engines [2], or that are useful for chemical process modeling. The materials and methods utilized for gathering the data used for property predictions are detailed in Sections 2.1 and 2.2, respectively, while the mathematical approach and uncertainty quantification are reported in Section 2.3 and 2.4, respectively.

2.1. Hydrocarbon reference materials

Sixteen hydrocarbon materials were sourced from three vendors and two fuel producers. These materials and their compositions were selected based on the ability to formulate a surrogate that would mimic many of the properties of Jet A/A-1. The final formulation of the mixture largely followed previous work on formulating surrogate compositions targeting aviation fuels [27–31]. Naturally, material purity, cost, and availability also played a role in these decisions. This blend is intended to represent the first-order properties of an aviation turbine fuel, not necessarily to mimic all relevant properties or exhibit all specification requirements of a Jet A/A-1. The details of the materials that were sourced are included in Table 1.

2.2. Gas chromatography and analyte detection

This work gathered data from a GCxGC-FID/VUV and compared it to results from a GCxGC-FID/MS system. Both units employed an FID for analyte quantification and split samples to another detector. Hydrocarbon type and carbon number distribution were determined on a Zoex thermal modulation system (GCxGC-MS/FID) with a previously reported method [3]. The MS for this system was not used. The GCxGC-MS/FID system was chosen as it had a calibrated hydrocarbon type template. The other GCxGC system (a GCxGC-VUV/FID), built upon an Agilent 8890, employed a flow modulation system with sample splitting to FID and a VGA-101 Vacuum Ultraviolet light detector (VUV). This detector and the associated analysis are further documented in Section 2.2.1. Flow modulation was maintained with a SepSolve INSIGHT modulator. A schematic of the GCxGC-VUV/FID system is illustrated in Fig. 2.

Table 1
Blended volumes, materials, purities, reference numbers, and suppliers for the reported surrogate.

Material name	Purity or POSF No.	Supplier	Blended vol. (23 °C), mL
Methylcyclohexane	99%	Sigma-Aldrich	2.2
cis-1,2-dimethylcyclohexane	98%	TCI	7.5
2,2,4-trimethylpentane	>99%	Sigma-Aldrich	7.5
1,2,4-trimethylcyclohexane	98%	Sigma-Aldrich	21.3
n-butylcyclohexane	99%	Alfa Aesar	10.5
iso-butylcyclohexane	>97%	TCI	10.5
trans-decahydronaphthalene	96.5%	MilliporeSigma	10.5
cis-decahydronaphthalene	98%	TCI	10.5
1-methylnaphthalene	96%	Alfa Aesar	26.8
n-undecane	>99%	Sigma-Aldrich	28.8
n-hexylbenzene	98%	Alfa Aesar	15.5
1,4-diisopropylcyclohexane	98%	Alfa Aesar	15.5
n-tridecane	>99%	Sigma-Aldrich	19
2,2,4,4,6,8,8-heptamethylnonane	98%	Sigma-Aldrich	5.05
ATJ (ASTM D7566 A5 [*iso*-butanol])	13718	Gevo	46.5
Farnesane	11832	Amyris	14.0

2.2.1. GCxGC-VUV/FID method

The GC temperature profile was initiated at a temperature of 40 °C, held for 6 s at 40 °C, increased at a rate of 2 °C per minute until a temperature of 280 °C was reached, and terminated. FID quantification for this GCxGC system used the INSIGHT ChromSpace software (Version 1.5.1). One μ L of the undiluted sample was injected with a Hamilton 10 µL syringe and a Merlin MicroShot manual injector at a split ratio of 300:1 and inlet temperature of 250 °C (Fig. 2a). The two-column setup used an SGE BPx5 with a stationary phase made up of 5% phenyl and 95% dimethyl polysiloxane as the primary column (Fig. 2b) and an SGE BPx50 with a stationary phase made of 50% phenyl polysilpenylene-siloxane as the secondary column (Fig. 2d). The primary column had a length of 20 m, an ID of 0.18 mm, and film thickness of 0.18 µm. The secondary column had a length of 5 m, an ID of 0.25 mm, and a film thickness of 0.10 µm. The connector line from the split plate to the FID and the VUV was 1 m long with an ID of 0.25 mm.

A modulation time of 4 s, a fill time of 3700 ms, and a flush time of 300 ms were used for the modulator. The primary column had a carrier gas flow rate of 0.75 mL/min of grade 5.0 helium sent through a Restek Triple Filter. The secondary column used a flow rate of 24 mL/min. The FID was set to 300 °C. The air (ultra-zero grade), H_2 (grade 6.0), and N_2 (grade 5.0) to the FID was set to 400, 40, and 25 mL/min, respectively.

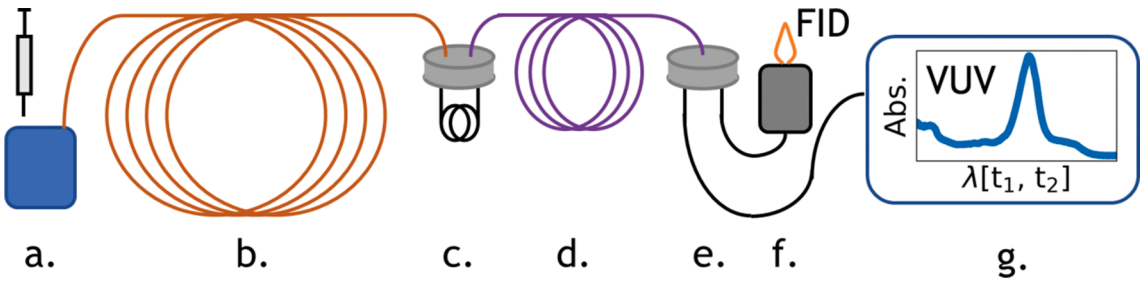

Fig. 2. Illustration of GCxGC-FID/VUV system. Samples are injected (a), travel through a primary column (b), flow modulation system (c), and a secondary column (d). The sample is then split (e) with a fraction going to a flame ionization detector (f) and a vacuum ultraviolet light absorption system (g). Additional valves and gas lines are not pictured here.

2.2.2. GCxGC-VUV/FID mass concentration determinations

Quantification was performed using FID response data and a set of blended calibration samples. Calibration samples were measured via relative response factors for each isomer individually. To do this, each species was tested in 4 blends at 4 different concentrations. Each individual blend had 4 species included, for a total of 16 calibration samples. Each species was blended by volume, but masses were recorded. Species for the calibration were blended at ratios of 20 μL/1080 μL, 50 μL/1200 μL, 50 μL/700 μL, and 100 μL/900 μL. The solvent used was dichloromethane. The calculated mass of these tests was compared to the TIC response, identifying a linear relationship between TIC and mass. These relationships were applied to each individual peak to convert from FID response to mass fractions. The peaks that were not within the calibration matrix were taken to be the average of the measured relationships. Peak areas were calculated using the integration tool built into Chromspace along with Top-hat noise cancellation. The integration method employed was a pseudo-Gaussian curve-fitting algorithm. The calibrations curves for analytes had R^2 values exceeding 0.998.

2.2.3. Vacuum ultraviolet analyte identification

A VGA-101 (VUV Analytics) was used to obtain vacuum ultraviolet absorption spectra and match to known spectra. Identification of analytes was made solely with the VUV/VGA-101, meaning no retention time information was used for matching. Two-dimensional separations were only used to isolate spectra, and retention times were ignored for matching. The detector measured the transmission of light between 125 nm and 430 nm and was recorded at 76.92 Hz. Signal averaging was accomplished during post-processing. At the interface between the VGA-101 and the gas chromatograph, the sample transfer line was maintained at a temperature of 250 °C. Reference materials described in Section 2.1 were used to augment the licensed reference library, and the spectra from these materials were gathered from a series of measured points in the absence of overlapping spectra. There, matching algorithms leveraged in-house code, which compares measured spectra to the reference library spectra. The matching method employed filtering to focus on regions of the spectrograph with significant absorptions while ignoring areas with a low signal-to-noise ratio. Matching reference spectra to measured spectra achieved a matching R^2 value > 0.99. Low signal-to-noise regions of the absorption spectra depend on the analyte type and concentration.

With internally constructed codes, time synchronization was accomplished to associate the VUV absorption spectra with FID signals. This software averaged vacuum ultraviolet light absorption spectra in two dimensions (t_1 and t_2), i.e., across multiple modulations. Here, the averaging over multiple modulations enables improved identification, as signal-to-noise reduction increases the confidence in matching spectra. The software used allowed for the selection of data away from coeluting analytes, negating the need for any signal deconvolution.

Figure 3 continues to illustrate the path from sample to final result with the flow of data acquisition to analyte quantification, classification, and identification. The signal from the FID (Fig. 3i.) is processed to two dimensions (Fig. 3ii.) where peaks are placed in the class bins with associated carbon numbers (Fig. 3iii.). Data from the VGA-101 (Fig. 3iv.) was similarly processed into two dimensions, and the signal for a given

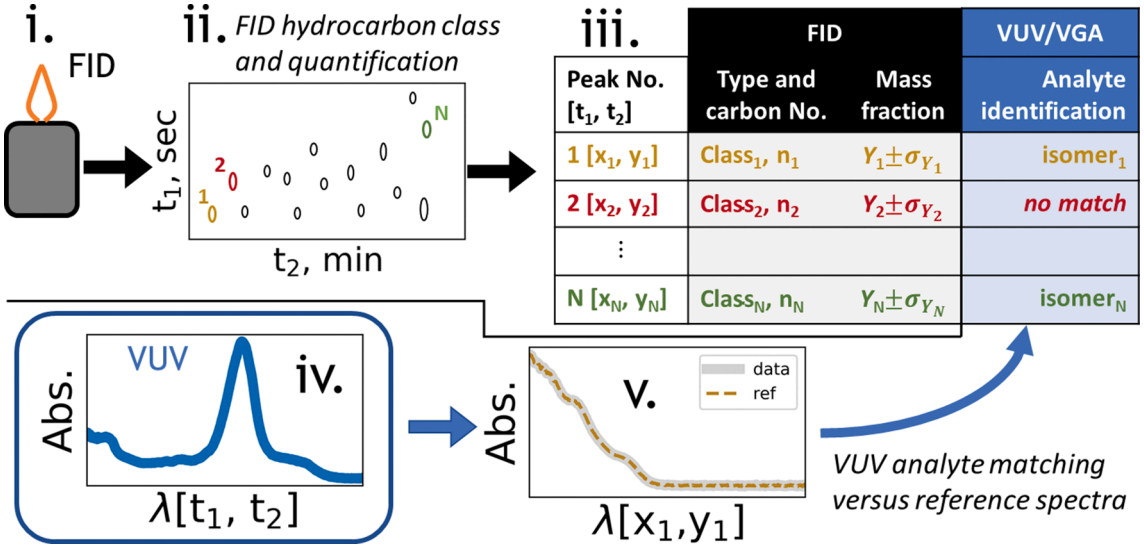

Fig. 3. Illustration of the path from data acquisition to quantification with FID (i.) and identification with VGA-101 (iv.). The two-dimensional FID peaks (ii.) are used to distinguish hydrocarbon types/empirical formulas for given peaks and the associated mass fractions (iii.). The VGA-101 absorption signal is matched to corresponding FID time stamps to identify specific species from reference data (v.).

peak averaged (Fig. 3v.). These averaged data were matched to reference data to identify the analyte. In some cases, analytes are not matched with reference spectra, and the specific isomer is unknown.

2.3. Mathematical approach

2.3.1. Database of hydrocarbon properties

Properties utilized in the study follow the previous work of Yang et al. [3], except that additional measurements have been made on individual components used in this study.

2.3.2. Blending rules

The blending rules for density, viscosity, surface tension, DCN, distillation curve calculations, freeze point, flash point, heat capacity, and thermal conductivity used here follow previous work in the lab on similar papers [3,30,32–34].

2.4. Uncertainty quantification

2.4.1. Sources of uncertainty considered

With the approach used here, uncertainties in property determinations came from three principal sources: UQ1) the measured concentration data (σ_{Y_i}), UQ2) the source property data from the NIST library and laboratory measurements (σ_{Z_i}), and UQ3) known-unknowns from analytes that are identified by class but not a specific isomer (σ_{isomer}) (i.e. the unidentified peaks in the FID measured concentrations such as analyte 2 in Fig. 3 where there is no VUV match).

- UQ1 Analyte quantification (σ_{Y_i}): The uncertainty of the concentration measurements was determined by considering the uncertainty arising from the calibration curves. While the calibration curves did achieve R^2 values > 0.998, there still exists some level of uncertainty regarding the actual concentration of the analyte. Here a normal distribution was assumed about the calibration coefficient, and values were randomly sampled about this distribution.
- UQ2 Root property data (σ_{Z_i}): Sourced property data uncertainties were used from the NIST database and the measurement uncertainties for individual compounds measured in the lab. Once more, the distribution of these properties was assumed to be normal. As described later regarding UQ3, individual properties for each analyte were randomly sampled before the individual properties were blended/modeled together.
- UQ3 Isomeric uncertainty (σ_{isomer}): In the event of analytes being below the limit of detection for the VUV or not currently identifiable when reference spectra are not available, the analyte was 'blinded,' as in no assumption towards its identification was made other than the determined hydrocarbon class and associated carbon number. In this event, all molecules in the database that fit the class and carbon number for that analyte peak were considered. Mathematically, σ_{isomer} for a given property is the uniform weighted distribution for all the isomers that fit the definition of a hydrocarbon class and carbon number ($\sigma_{isomer} = f(Z_i \pm \sigma_{Z_i}\ \forall i \in [\text{Class}_j, n_j])$), where j is determined from the FID data). The uncertainty is calculated as the impact for all isomers in the class and carbon number, and a specific example is given later in the text. This uncertainty term is typically the largest of the three uncertainty terms [10]. The impact of this term has tended to have the most dramatic impact on properties that have a significant variance for a given class and carbon number (e.g., viscosity), see Yang et al. Fig. 2b [3].

The uncertainty of the concentration measurements and the individual constituent property data was represented in these predictions by an assumed normal distribution. In contrast, the uncertainty arising from the unidentified analytes was captured by random sampling of all species within the library that are eluted into the same GCxGC bin and not further parsed via VUV spectral data. These three uncertainty components were determined individually, in parallel, and collectively in separated Monte Carlo simulations to parse out the contribution from each source.

The three types of uncertainty and the general computational approach are described below and illustrated in Fig. 4. Data and identification information (Fig. 4A) was linked to the property database (Fig. 4B). Analytes that were not identified were 'blinded', as shown for analyte/peak number 2. There analyte 2 was not assumed to be any specific isomer. Instead, all isomer candidates that meet the limiting class and carbon number for that peak were considered. For example, if analyte 2 was a ten carbon *iso*-alkane, all 73 ten carbon *iso*-alkane isomers would be used for the prediction sequence. In that prediction sequence, a specific mass fraction (UQ1) (Fig. 4A), isomer (UQ3) (Fig. 4A), and associated property (UQ2) (Fig. 4B) are selected. UQ1 and UQ2 are selected using uncertainties and assumed normal distributions. The specific isomer for unidentified analytes is selected from a uniform distribution at random, as illustrated in Fig. 5. In the event that a specific property is not known or can't be calculated, random isomers and their associated properties are used as done in UQ3. In Fig. 4, this is illustrated in B. with the LHV of the *N*th analyte. There the LHV is unknown for the *N*th species, and all the isomers in that hydrocarbon class are sampled. This was the same process that was done for all properties associated with the second peak/analyte for where all properties are randomly sampled. The associated properties were then combined via a blending rule. The sequence of mass fraction, property, and isomer sampling was repeated at least 10,000 times until the predictions converge (Fig. 4C), i.e., reach an apparent asymptote. These statistics are then communicated in the aggregate (Fig. 4D). Fig. 4D shows 10,000 Lower Heating Value (LHV) predictions (Ind. Predictions) with all three uncertainties included. The aggregate in Fig. 4D communicates the mean value for all 10,000 predictions (open circle), the 68% confidence interval (CI) (solid blue line), and the 95% CI (capped dashed line). The sequence reported here was completed for each property.

2.4.2. Monte Carlo sampling

Many (at least 10,000) predictions were evaluated for every property and, where reported, each temperature condition. Predictions were repeated until a corresponding histogram of outcomes had a smooth profile, where the histogram bin size was 10% of the precision of the corresponding measurement method or less. For example, the repeatability of the derived cetane number is 0.81 for a derived cetane number of 43, the derived cetane number of the surrogate here. The histogram bin size for this property is 0.08 derived cetane number.

Uncertainties for variance resulting from the inability to identify a given species (UQ3, σ_{isomer}) follow the method reported by Yang et al. [3], with a key distinction being the addition of VUV identification. In the work of Yang et al., all of the carbon detected via FID was randomly assigned to a specific isomer in the hydrocarbon database that has similar volatility and polarity to the detected carbon or a class-carbon number combination. Here, a majority of that carbon was able to be assigned to specific isomers. The remaining unidentified carbon was assigned to random isomers just like the previous method. All assignments were assumed here to be correct, although it is understood that some analyte spectra in future work may be similar to two or more spectra in the reference library of spectra. While this was not the case for any of the principal components in the surrogate fuel created for this work, the generalization of this approach to more complicated mixtures of hydrocarbons will have to include each of the probable matches in the Monte Carlo simulation of the mixture. Relative to FID alone, for which a detected peak could be any of 100's of possible isomers, the identification here reduces uncertainty substantially.

Species concentration uncertainties (UQ1) were determined from multiple experiments using a more complex hydrocarbon mixture. The terms used to calculate the repeatability included the hydrocarbon type-carbon number bins, measurements from experimental data, and the associated calibration curves, applied to a more complicated mixture

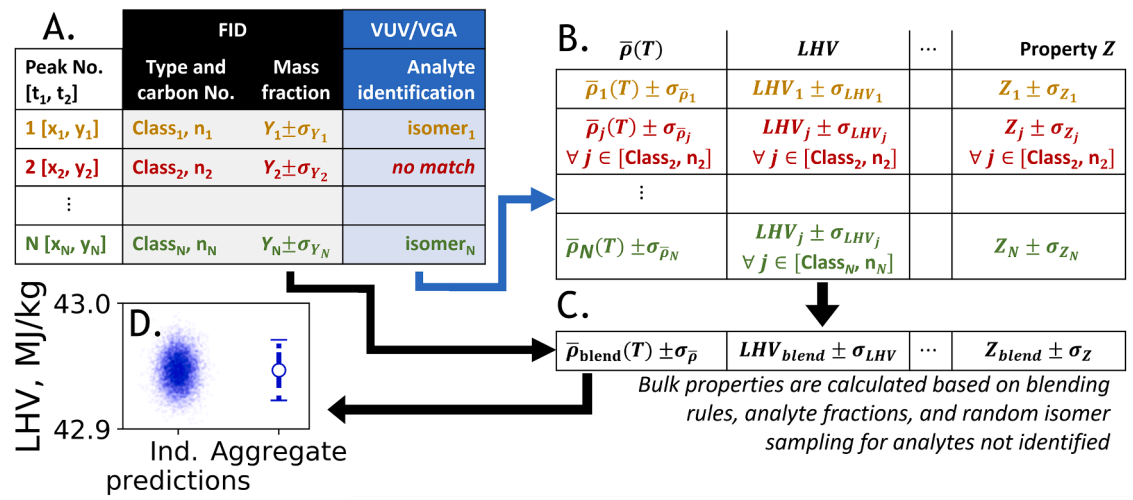

Fig. 4. Illustration of computational approach incorporating data generated, properties from the database, and incorporating various types of uncertainty. The data from the FID and VUV/VGA-101 (A) are coupled to a database (B). The blend properties (C) are calculated from individual properties and all three sources (property uncertainty, σ_Z; measurement uncertainty, σ_{Y_i}; isomeric uncertainty, σ_{isomer}) of uncertainty considered. Properties are calculated thousands of times while sampling from uncertainty distributions, and the aggregate is reported (D).

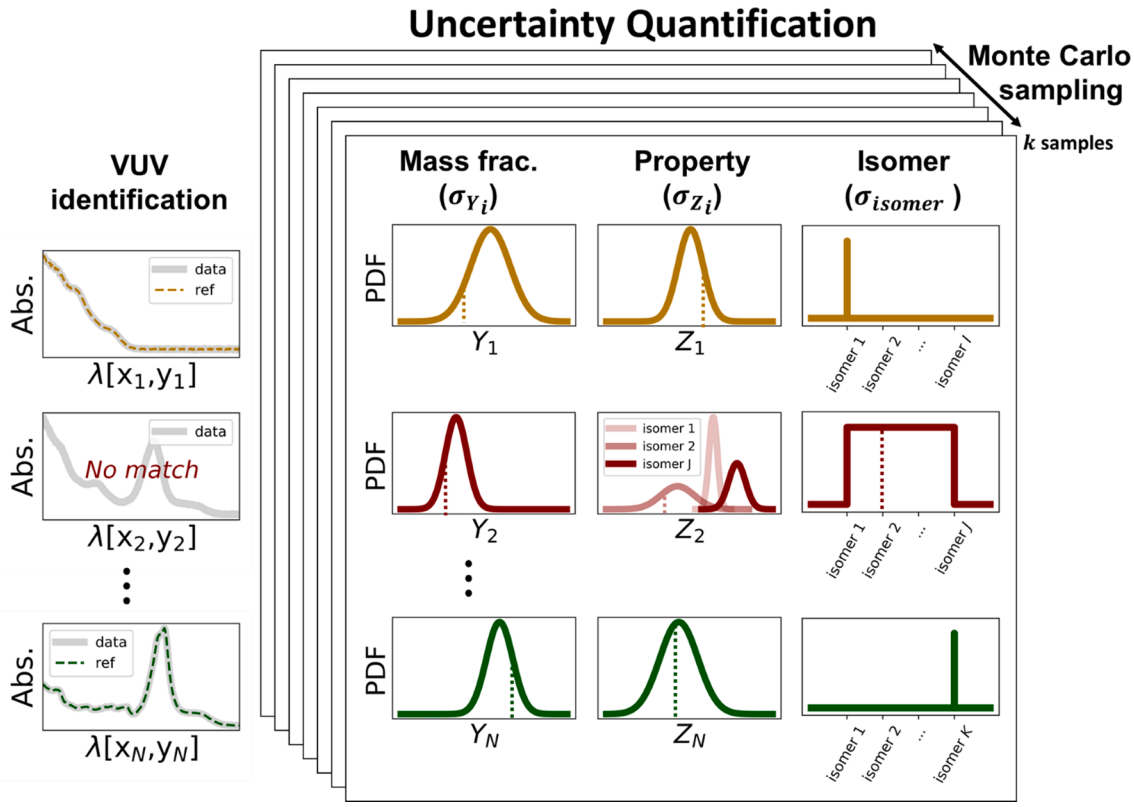

Fig. 5. Illustration of one Monte Carlo sampling sequence and the types of uncertainty considered here.

(JP-8, POSF 4751). The reproducibility of hydrocarbon type-carbon number bins used here was (σ = 0.03 to 0.07 m%) depending on the hydrocarbon type-carbon number. This reproducibility, as part of UQ1, was sampled when developing the blended property predictions. The repeatability of the measurements for reference samples was incorporated into property prediction variance. Measurement repeatability variance (UQ2) from viscosities, densities, surface tensions, flash points, and freeze points for reference materials reported in Section 2.1 were incorporated into the property predictions in this paper's Results and discussions section.

An illustration of the described uncertainty quantification is reported in Fig. 5. For each Monte Carlo sample, a random value was sampled on the mass fraction and property distribution for all analytes and all properties (vertical dotted lines). In Fig. 5 the first and *N*th peaks are identified, and the second peak is not, as illustrated in the absorbance versus wavelength plots (λ). Correspondingly, the isomeric uncertainty (UQ3) for the first and *N*th analyte is zero for all Monte Carlo samples. The second analyte, however, is not known. A random isomer that belongs in the corresponding class and carbon number is sampled for each Monte Carlo simulation. A specific property value (vertical dotted line)

is then sampled for each property distribution. The middle plot illustrates several property distributions for the second analyte here. In this example, the second isomer in the bin is selected, and a random property value on the distribution for property Z is assigned. The bulk property (Z) is then predicted for each simulation, k times. The k property predictions then are aggregated into CIs, like shown in Fig. 4D.

3. Results and discussion

3.1. Identification and quantification

The bulk composition of the surrogate hydrocarbon type analysis is found to be composed of 98.7 m% in 9 major bins (>1.0 m%) and carbon numbers from seven (C7) to sixteen (C16), reported in Table 2. A chromatogram of the GCxGC-VUV/FID is reported in Fig. 6. The remaining composition of the fuel is composed of small amounts of alkenes from Amyris (0.3 m%), C20 *iso*-alkanes from Gevo (0.3 m%), and other small (<0.05 m%) concentrations of contaminants in procured solvents used for blending. A chromatogram is reported in Fig. 6 and the composition of the significant fractions is found in Table 3. Fig. 7 illustrates the method for identifying analytes from measured data with the VUV detector. Fig. 7a illustrates the measured absorbance of a peak (black circles) and the matched reference spectra to that peak (solid line). The spectra in Fig. 7a is matched best to 2,2,4-trimethylpentane (i.e., *iso*-octane). For reference, 2,2,3-trimethylpentane reference spectra (dashed line) is also plotted illustrating the clear identification of 2,2,4-trimethylpentane as compared to another structural isomer. The remaining subplots in Fig. 7 (b, c, and d) illustrate the identification of molecules with one additional methyl group (b), stereoisomers trans- and *cis*-decalin (c), and clear spectral response of aromatics versus aliphatic molecules (d).

Table 2
Carbon numbers, hydrocarbon class, isomers in the corresponding class, and carbon number, identified molecules in the sample, and measured concentrations for bins and individual peaks exceeding 1 m%.

Hydrocarbon Class, GCxGC-FID/MS	Isomers in Class, (-)[†]	Hydrocarbon Molecules, GCxGC-VUV/FID (Fig. 6 ref.)	MS/FID |VUV/FID, m% [††]
C7 *cyclo*-alkanes	4	Methyl cyclohexane (ii.)	1.15|1.08
C8 *iso*-alkanes	17	2,2,4 Trimethyl pentane (i.)	2.81|2.72
C8 *cyclo*-alkanes	≥ 37	cis 1,2 Dimethyl cyclohexane (iii.)	3.15|2.77
C9 *cyclo*-alkanes	≥ 53	1,2,4-trimethylcyclohexane stereoisomers (iv. and v.)	8.67|8.14
C10 *cyclo*-alkanes	≥ 70	n-butylcyclohexane (viii.)	8.32|3.90
		iso-butylcyclohexane (vii.)	4.94
C10 dicyclo-alkanes	≥ 7	*cis*-decalin (xi.)	9.32|4.70
		trans-decalin (ix.)	4.25
C11 di-aromatic	2	1-methylnaphthalene (xvii.)	13.70|12.86
C11 n-alkane	1	n-undecane (x.)	9.89|10.98
C12 alkyl benzenes	≥ 58	n-hexylbenzene (xiv.)	6.30|6.82
C12 *iso*-alkanes	354	2,2,4,6,6-pentamethylheptane (vi.)	12.54|9.61
C12 *cyclo*-alkanes	≥ 38	1,4-diisopropylcyclohexane stereoisomers (xii. and xiii.)	6.04|5.91
C13 *iso*-alkanes	801	Not resolved	1.04|———
C13 n-alkane	1	n-tridecane (xv.)	6.57|6.87
C15 *iso*-alkanes	4,346	Farnesane (xviii.)	4.79|5.43
C16 *iso*-alkanes	10,359	2,2,4,4,6,8,8-heptamethylnonane (xvi.)	4.40|2.99
Total			98.69|93.96

[†]The number following the ≥ symbol corresponds to the number of isomers in the NIST database that are part of the stated hydrocarbon class and used in this study. The total number of possible isomers is greater than or equal to this value reported.
[††]The first number is species class concentration data provided by the GCxGC-FID/MS. The second number is identified species concentration measurements made by GCxGC-VUV/FID.

The concentrations of the sample material are found to be near the typical range for conventional fuels [35], with the exception of diaromatics. Within this type, C11 diaromatics are found to have the highest concentration, at 13.7 m%. A comparison of the surrogate studied here in contrast to a representative Jet A/A-1 reported by Edwards is shown in Fig. 8. The carbon distribution for an average Jet A/A-1 (green filled bars) is compared to the distribution of the surrogate studied here (thin color mapped filled bars), with the average carbon numbers for those correspondingly reported. The bulk chemical composition of the surrogate is found to have a molecular weight of 152 gm/mol, a hydrogen content of 13.5 m%, and an average empirical formula of $C_{10.9}H_{20.3}$. The 'average' Jet A in the Edwards study reported a molecular weight of 159 gm/mol and hydrogen content of 14.0 m% [35]. The motivation in the selection and composition of this surrogate is not to mimic combustion property targets or develop a fully drop-in conventional fuel. Instead, the motivation, as seen later, is to illustrate a method to dramatically reduce the uncertainty of predicting key operability properties for sustainable aviation fuel candidates in prescreening, develop bottom-up property models for computational fluid dynamics, and other novel applications.

Vacuum ultraviolet absorption spectra identified 16 individual analytes with a carbon balance of 93.96 m%, see Table 2. One prominent C13 *iso*-alkane peak (1.03 m% by GCxGC-FID/MS) is unidentified by VUV. Other minor unidentified peaks are heavy (>C16) n- and *iso*-alkanes, and several alkenes are observed in low concentrations. The class and carbon number concentrations determined by the GCxGC-FID/MS approach [3] should be greater than or equal to those determined by GCxGC-FID/VUV in Table 3. The former integrates carbon over a region that includes all isomers in the bin, while the latter (so far) integrates carbon within visible peaks only. Two notable inconsistencies between the two GCxGC systems for mass concentrations are observed. A greater mass fraction is found in the n-undecane and farnesane peaks in the VUV system versus the other system. Since these molecules are directly calibrated in the VUV system, it is unlikely to have any issues with molecule identification at the time of this study.

3.2. Property predictions

Several properties for the surrogate are predicted and compared to measured values, and several additional properties, for which no experimental data are available, are also predicted. The set of predicted properties is not intended to be illustrative of restrictions to future work. However, the diverse set of properties is predicted here to illustrate the reach and future potential of the analytical, diagnostic, and numerical approach employed here. The properties selected here follow the National Jet Fuels Combustion Program (NJFCP) results for prescreening sustainable aviation fuel candidates [2,36–38]. Those property predictions are reported in Figs. 9, 10, and 11. These NJFCP facing properties have been identified to constrain the operability variance of sustainable aviation fuels to within the experience range of conventional fuels. Fig. 9 compares an experience range of conventional fuels (green shaded region) and specification limits (red lines and regions) to measurements and predictions. (Note that the DCN is not specification property for aviation fuel, but the DCN has been identified as necessary for combustor operability compliance [36,39].) The measurements (black circles) are reported with their corresponding ASTM reproducibility or effective 95% CIs (black lines). Measurements for these properties are in the range of conventional fuel requirements with the exception of the flash point, which is below the 38 °C requirements [40]. Similarly, the Tier Alpha predictions (blue open circles) are reported with their corresponding 68 and 95%CI (solid and capped-dashed lines, respectively). Predictions leveraging VUV identification (Tier Alpha + VUV, red left triangle) are reported with their corresponding 68 and

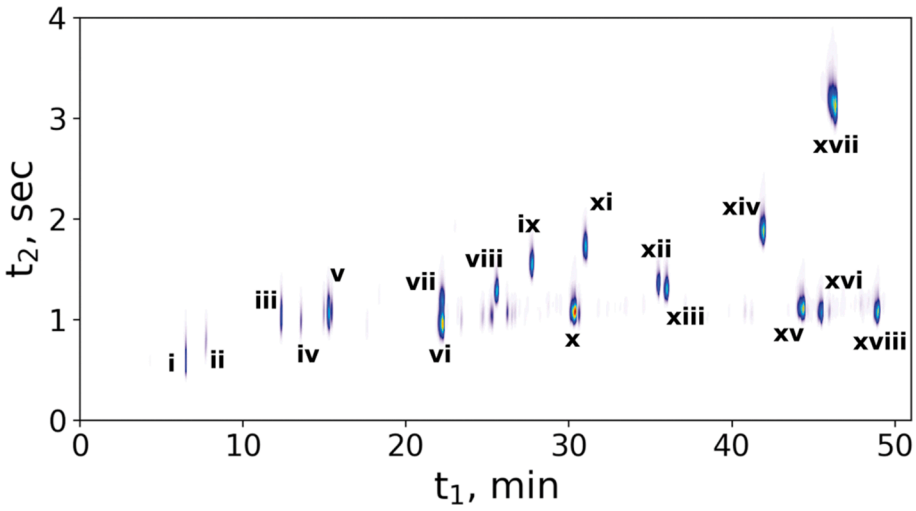

Fig. 6. Chromatogram of surrogate in the GCxGC-VUV/FID. Analyte identifications can be referenced in Table 2 with roman numerals.

Table 3
Hydrocarbon concentrations of surrogate in this study compared to a representative Jet A/A-1 (POSF 10325).

Hydrocarbon class	This study, m%	Ref. Jet A/A-1, m%
alkylaromatics	6.4	12.9
diaromatics	13.7	2.3
iso-alkanes	26.2	29.7
n-alkanes	16.5	20.0
monocycloalkanes	27.5	25.1
dicycloalkanes	9.4	6.6

95% CIs (solid and capped-dashed lines). The LHV predictions include the lowest possible LHV value (star). This lowest possible value provides a range of probabilistic values (i.e., capped-dashes [95%CI], solid lines [68%CI], and symbols [most probable]), as well as the lowest possible LHV value (star) for the given hydrocarbon classes and carbon number distribution. Further discussion on LHV determinations and measurements can be found in a contribution by Boehm et al. [10].

All predictions in Fig. 9 agree with the measured values. However, leveraging the VUV identification, the average absolute error between the measurements decreased by more than two times. The average absolute percent difference between the blind Tier Alpha (FID only) and Tier Alpha + VUV methods is 4.99 and 2.24%, respectively. Perhaps most notably, the uncertainty associated with the two approaches dropped significantly when the VUV/VGA system is employed. The 68 and 95% CI between the two prediction methods for surface tension is reduced up to 21 and 18 times, respectively. However, the freeze point and DCN confidence intervals between the two methods are modestly reduced. UQ2 for the freeze point and DCN, or the uncertainty associated with the specific molecular properties, is considerable. Additionally, the variance for these properties for a given class and carbon number (UQ3, σ_{isomer}) is, once more, significant. For example, consider the DCN variance between n-octane and *iso*-octane, or the fact that an iC8 isomer (2,2,3,3-tetramethyl butane) is a solid at room temperature; while other iC8 isomers freeze below −90 °C. The LHV predictions illustrate that the specific isomers selected in this study have a significantly lower LHV than the average molecule in their classes.

The distillation curve (Fig. 10) is estimated from the mass concentration measurements by calculating vapor pressure throughout the integration of mass loss from the system. The initial boiling point is the temperature at which the vapor pressure equals one bar, and it marks the beginning of the simulation range. At that point, a small increment of mass is removed from the system in a proportion equal to the partial pressure of each constituent. Upon removal of the first increment of mass, the mole fractions of each component in the liquid phase are updated, and a new boiling point is determined. This integration continues until no mass is left in the system. An alternative numerical method for boiling range distribution of petroleum fractions by gas chromatography is described in ASTM D2887. No claim is made here regarding which of these two methods is a more accurate predictor of a real distillation, such as ASTM D86. However, the method described above is more convenient for uncertainty analyses arising from UQ1, UQ2, and UQ3. The distillation simulation via ASTM D2887 (black circles and line) is compared with the current determination method (solid red line) in Fig. 10, with the predictions estimated 95% confidence interval (shaded region). The two numerical methods are in fair agreement with each other, although the light fraction deviates the most substantially. Similar to Fig. 9, a range of conventional Jet A/A-1 fuels (green shaded region) and the ASTM D1655 specification limits (red line and shaded region) are provided as a reference.

Densities and viscosities for the surrogate are reported in Fig. 11. Measured (black circles), blind Tier Alpha predicted (blue line), and Tier Alpha + VUV predicted (red line) are compared over a range of relevant operability temperatures for jet fuels [42]. The corresponding prediction uncertainties are reported for the Tier Alpha (blue shaded regions) and Tier Alpha + VUV (red shaded regions). An excellent agreement between both prediction methods and the density measurements is observed. There is a modest difference noticed for each of the three slopes (i.e., $\Delta\rho/\Delta T$) reported. The percent difference between the measured density gradient and the Tier Alpha + VUV prediction is + 0.8%, while the percent difference between the Tier Alpha and the measured slopes is + 3.0%. The modest but distinguishable slopes make the Tier Alpha density predictions higher/lower than the measured values at the lowest/highest temperatures.

The most noticeable difference between the two predictions for density is the dramatic reduction of uncertainty in the predictions. The decrease in isomers, considered for UQ3 and illustrated in Fig. 5, led to substantially smaller CIs in the case of the Tier Alpha + VUV predictions compared to Tier Alpha alone. Numerically, the addition of the VUV identification reduced the 95% CI range from an average of 24.8 kg/m^3 (Tier Alpha +/- 2σ) to 1.70 kg/m^3 (Tier Alpha + VUV +/- 2σ). For comparison, the experimental ASTM D4052 reproducibility for the density measurement is reported as 2.7 kg/m^3 at −20 °C, while the experiment's reproducibility is reported as 0.5 kg/m^3 (Anton Paar, SVM 3001). In this study, most of the individual molecules are measured directly. Thus $2\,\sigma_{\rho_i} = 0.5$ kg/m^3 for those compounds measured directly. For reference, the NIST reported uncertainty for a representative molecule (2-methyl decane) at −20 °C is 2.92 kg/m^3.

Similarly, the viscosity predictions compare well to the measured

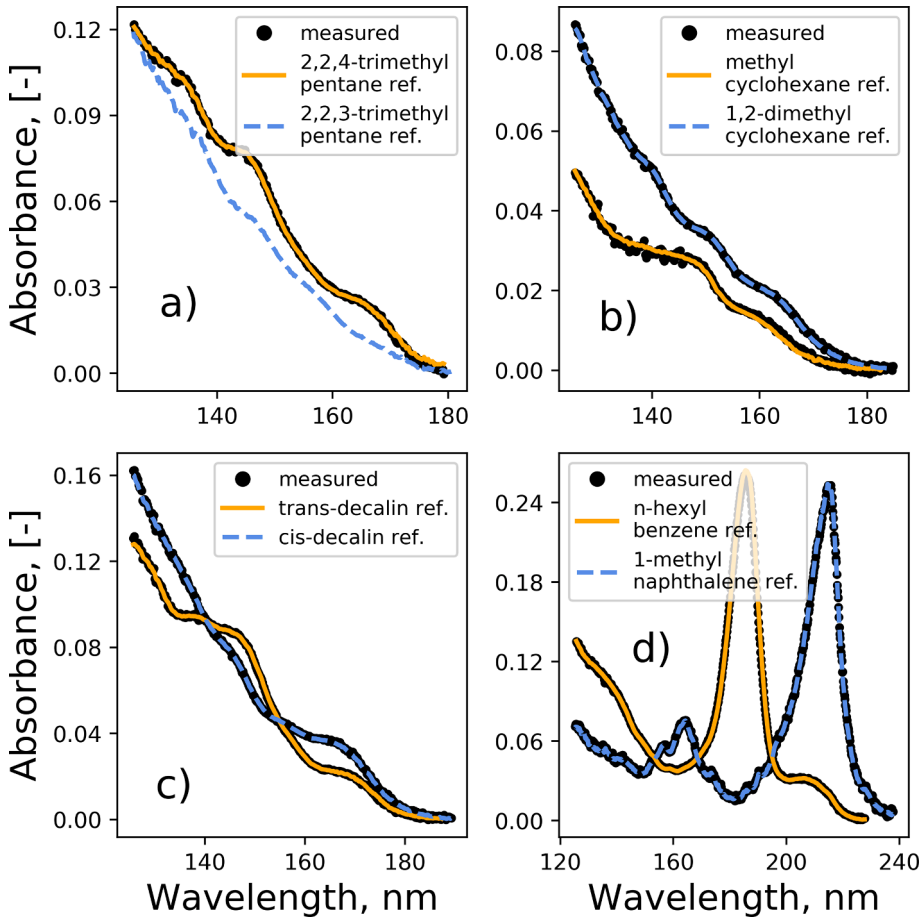

Fig. 7. Comparison of VUV absorbance of sample analytes (symbols) as compared to reference spectra (dashed and solid lines). VUV absorption spectroscopy identifies the analytes in this study in comparison to some similar structures.

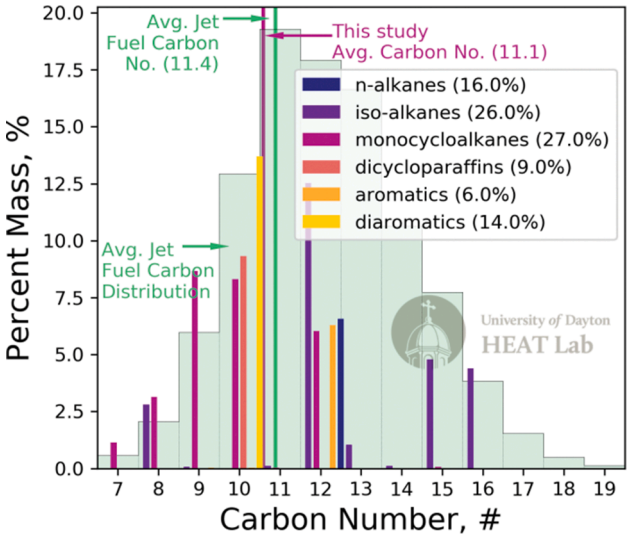

Fig. 8. Comparison of carbon number distribution and average carbon number for an average Jet A/A-1 and the surrogate studied here.

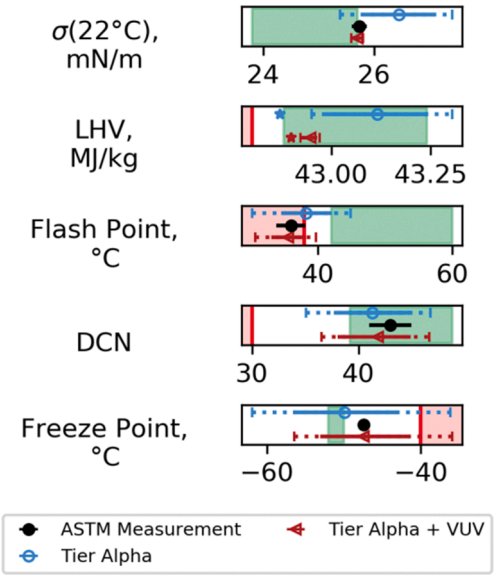

Fig. 9. Comparison of the current method (red symbols and lines) with the previous method (blue symbols and lines). Nominal values as determined by an ASTM standard method for direct property measurement as shown (black symbols) for reference. Fuel specification limits are denoted by a vertical red bar. The green shaded region shows the range of values known for petroleum-derived fuels. The red shaded region corresponds to 'out-of-spec.' (The reader is referred to the web version of this article for color references.)

values. The most probable Tier Alpha and Tier Alpha + VUV predictions vary between 1.6 and 70% and −1.0 to 6.8% error as compared to the measured values, with the experimental repeatability for the measurements reported as 0.35%. The Tier Alpha viscosity prediction 95% CI overlaps with the measurement values for the entirety of the

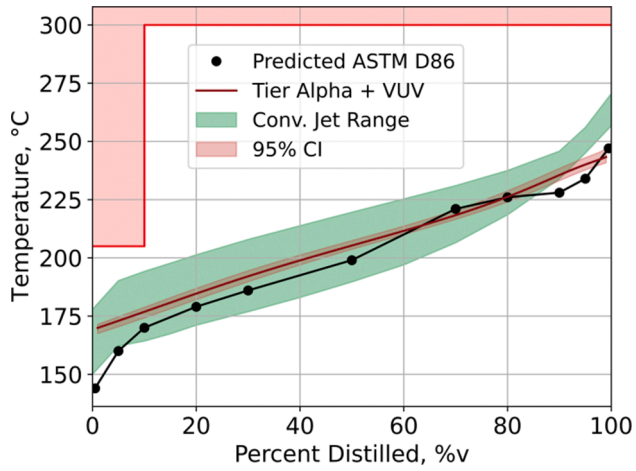

Fig. 10. Measured (ASTM D2887 to predicted D86) and VUV predicted distillation temperatures. The prediction is made using vapor pressure values from NIST and vapor–liquid equilibrium calculations to determine calculate predicted ASTM D86 distillation temperatures.

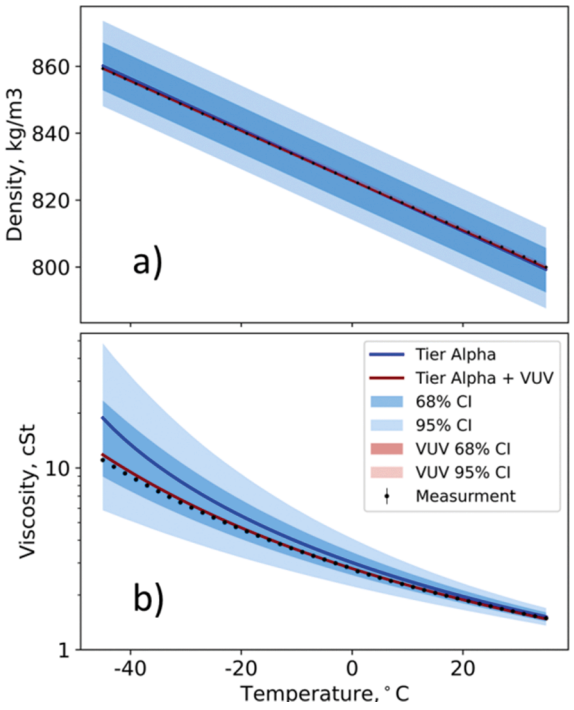

Fig. 11. Predicted and measured densities (a) and viscosities (b) for a range of relevant jet fuel conditions. Measurements and their uncertainties are shown with black-filled circles. The FID only Tier Alpha predictions are shown as solid blue lines, with the corresponding shaded regions illustrating the 68 (dark blue) and 95% CI (light blue). The prediction leveraging the VUV data is illustrated by a solid red line and corresponding red-filled areas. (The reader is referred to the web version of this article for color references.)

temperature range. However, the Tier Alpha + VUV nominal predictions agree with measurements at temperatures above −21 °C within the uncertainty of the measurements. The variance between the measurements and predictions is the motivation for higher fidelity models and quantifying predictive error, i.e., the addition of a fourth uncertainty quantification (UQ4, σ_{model}). As evident in the plot, the model uncertainties are substantially reduced with the inclusion of the VUV identification.

Two additional properties are reported as an illustration of the current and ongoing capability of leveraging VUV identification to predict bottom-up properties of mixtures. Fig. 12 plots predictions for the Tier Alpha (blue line and shaded regions) and Tier Alpha + VUV (red line shaded areas) thermal conductivity (a) and heat capacity (b) over a range of temperatures. The thermal conductivity predictions are found to be in near-complete agreement with each other. Similar to the previously reported predictions, the Tier Alpha + VUV prediction uncertainties are reduced. Interestingly, the uncertainty reductions there are modest, suggesting that the isomer uncertainty (UQ3) is not the dominant source of uncertainty with this property. The heat capacity predictions for the two methods are found in good agreement. Similar to the observation with the thermal conductivity, the uncertainty is not reduced substantially with the addition of the VUV identification, again implying that the predominant source of uncertainty is the root property data (UQ2, $\sigma_{\text{thermalconductivity}_i}$).

As mentioned previously, gradients of key properties for evolved material from solution can impact gas turbine operability. This has been observed and documented with preferential vaporization [18]. Fig. 13a predicts the DCN of the evaporated fraction for a fraction of material distilled. The nominal DCN value is predicted to rise from ~ 36 to a maximum of ~ 44 and fall to approximately ~ 43. The initial low value in the DCN value is from the evaporation of mostly methylcyclohexane and *iso*-octane, as the calculated DCN value represents the evaporated fraction. The corresponding rise in DCN is from the increasing fraction of higher DCN species evaporating. Finally, the drop in DCN at high distillation fraction is from the evaporation of heavy aromatics species (i.e., 1-methylnapthalene). The uncertainty illustrated in Fig. 13a represents the uncertainty of the vapor pressure calculations (UQ2), reproducibility in root DCN measurements (UQ2), and mass fraction uncertainties (UQ1). The uncertainty there does not include isomeric uncertainty (UQ3), as is included in Fig. 9. Absent the isomeric uncertainty, the uncertainty of the predictions is near the uncertainty of the measurements as the vapor pressure and mass fraction uncertainties are minimal compared to the ASTM D6890 reproducibility. Fig. 13b compared predicted volume concentrations of the liquid volume versus percent distilled. Table 3 can be used as a reference for identifying the various molecules referred to in Fig. 13b with the colored legend. The concentrations in the table are the values intersecting the left y-axis.

4. Conclusions

Advances in analytical chemistry experimentation and computation can advance the characterization of aviation fuels, the fidelity of computational fluid dynamic models, and the ability of fuel producers to model reactor behavior at low volumes. A novel approach to predict key aviation fuel properties and uncertainties with GCxGC-VUV identification has been reported. The approach was applied to a surrogate fuel with a reduced number of chemical constituents. Properties were predicted for the surrogate, and when possible, compared to measurements. Many properties were predicted with the previously reported method of Yang et al. and compared to the method of this study (i.e., with VUV). Nominal property predictions improved with the VUV identification. However, the most substantial improvements made with the new method was in the reduction of uncertainty. Using the VUV, the uncertainty associated with isomeric variance reduced substantially, as ~94 m% was identified in the surrogate. Beyond measured properties, the experimental and computation method was expanded to include heat capacity and thermal conductivity properties. Once again, the uncertainty of those predictions was reduced. Finally, the method was used to predict the DCN of the surrogate with respect to the distillation fraction of the fuel. There it was predicted for this sample that the DCN could increase and decrease over the distillation curve. This behavior, known as preferential vaporization, has been shown to be important near lean blowout in gas turbine combustors.

Applying this experimental method (GCxGC-VUV) to more complex mixtures, i.e., conventional fuels, will be more difficult than for the

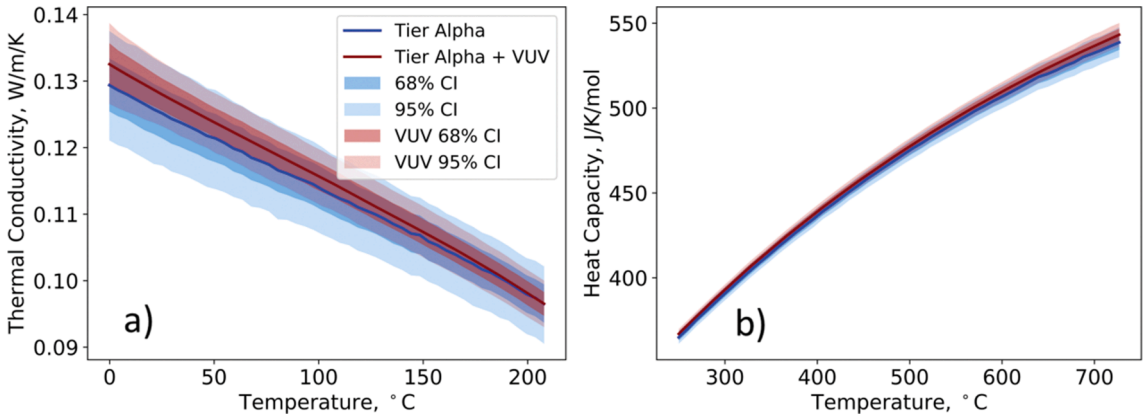

Fig. 12. Predictions of thermal conductivity and heat capacity with respect to temperature for Tier Alpha (blue line and shaded regions) and Tier Alpha + VUV predictions (red line and shaded regions). (The reader is referred to the web version of this article for color references.)

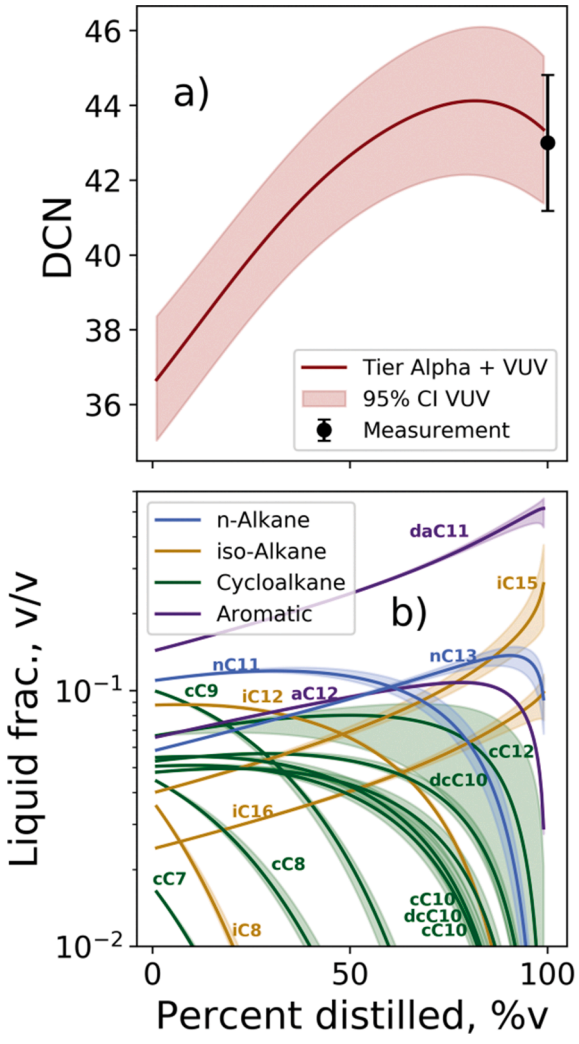

Fig. 13. Illustration of (a) the DCN prediction for the surrogate used in this study versus the distillation fraction and (b) the volume fraction of the remaining sample by percent distilled. Hydrocarbon types are denoted with a 'i,' 'a,' 'n,' and 'c' for *iso*-alkanes, aromatics, n-alkanes, and cycloalkanes, with the number after the 'C' denoting the carbon number of the species. Diaromatics and dicycloalkanes are denoted with a 'd.'

mixture reported here. However, the majority of carbon (~80 m%) is found in 186 peaks for a typical conventional Jet A (POSF 10325), while > 1123 other molecules compose the remaining faction. In short, 80% of the mass is contained in 21% of the analytes. At present, the VUV database used for this study has 242 spectra for molecules in the jet range, with additional spectra available. Questions remain regarding whether carbon balances nearing 80% are sufficient for constraining the properties reported here, additional properties of interest, and if it is possible to positively identify all or most of the 186 major peaks in POSF 10325.

Applying the numerical method to more complex mixtures has been done previously for a wide range of aviation fuels and blend components [3]. The predictive fidelity and uncertainty of the numerical method, as illustrated here and in Boehm et al. [10], will depend upon the accuracy of database properties and the models that articulate molecular properties to bulk mixture properties, in addition to the identification of isomers or the reduction of UQ3. Future work to predict properties from GCxGC-VUV measurements will need more spectra, specific columns and GC test methods tailored for the VUV, and possibly the calibration of the unit to subtle changes in isomer retention times, as the strength of the method has been shown to reduce the isomeric uncertainty of the analytes.

Funding

The authors would like to acknowledge funding from the U.S. Federal Aviation Administration Office of Environment and Energy through ASCENT, the FAA Center of Excellence for Alternative Jet Fuels and the Environment, project 65 through FAA Award Number 13-CAJFE-UD-026 (PI: Dr. Joshua Heyne) under the supervision of Dr. Anna Oldani. Any opinions, findings, conclusions, or recommendations expressed in this material are those of the authors and do not necessarily reflect the views of the FAA or other sponsors. Additional support for this paper was provided by US DOE BETO through subcontract PO 2196073.

CRediT authorship contribution statement

Joshua Heyne: Conceptualization, Formal analysis, Methodology, Funding acquisition, Project administration, Resources, Supervision, Visualization, Writing – original draft, Writing – review & editing. **David Bell:** Formal analysis, Methodology, Software, Visualization, Writing – original draft, Writing – review & editing. **John Feldhausen:** Formal analysis, Methodology, Software, Visualization, Writing – original draft, Writing – review & editing. **Zhibin Yang:** Formal analysis, Methodology, Software, Visualization, Writing – original draft, Writing – review & editing. **Randall Boehm:** Formal analysis, Methodology, Supervision, Visualization, Writing – original draft, Writing – review &

editing.

Declaration of Competing Interest

The authors declare that they have no known competing financial interests or personal relationships that could have appeared to influence the work reported in this paper.

Acknowledgements

The authors would like to acknowledge the support of Ms. Linda Shafer of the University of Dayton Research Institute (UDRI) for providing the GCxGC-MS/FID hydrocarbon type analysis. Additionally, we thank conversations with Mr. Richard Striebech of UDRI and Ms. Shafer regarding GCxGC methods.

References

[1] Huq NA, Hafenstine GR, Huo X, Nguyen HM, Stephen T, et al. Towards net-zero sustainable aviation fuel with wet waste-derived volatile fatty acids. Proc Natl Acad Sci 2021.
[2] Heyne J, Rauch B, Le Clercq P, Colket M. Sustainable aviation fuel prescreening tools and procedures. Fuel 2021;290:120004. https://doi.org/10.1016/j.fuel.2020.120004.
[3] Yang Z, Kosir S, Stachler R, Shafer L, Anderson C, Heyne JS. A GC × GC Tier α combustor operability prescreening method for sustainable aviation fuel candidates. Fuel 2021;292:120345. https://doi.org/10.1016/j.fuel.2021.120345.
[4] Hall C, Rauch B, Bauder U, Le Clercq P, Aigner M. Predictive capability assessment of probabilistic machine learning models for density prediction of conventional and synthetic jet fuels. Energy Fuels 2021;35(3):2520–30.
[5] Wang Y, Cao Y, Wei W, Davidson DF, Hanson RK. A new method of estimating derived cetane number for hydrocarbon fuels. Fuel 2019;241:319–26. https://doi.org/10.1016/j.fuel.2018.12.027.
[6] Vozka P, Modereger BA, Park AC, Zhang WTJ, Trice RW, Kenttämaa HI, et al. Jet fuel density via GC × GC-FID. Fuel 2019;235:1052–60. https://doi.org/10.1016/j.fuel.2018.08.110.
[7] D02 Committee. ASTM D2887 - Standard Test Method for Boiling Range Distribution of Petroleum Fractions by Gas 2021:1–35. doi:10.1520/D2887-19AE02.2.
[8] Ahmed A, Goteng G, Shankar VSB, Al-qurashi K, Roberts WL, Sarathy SM. A computational methodology for formulating gasoline surrogate fuels with accurate physical and chemical kinetic properties. Fuel 2015;143:290–300. https://doi.org/10.1016/j.fuel.2014.11.022.
[9] Govindaraju PB, Ihme M. Formulation of optimal surrogate descriptions of fuels considering sensitivities to experimental uncertainties. Combust Flame 2018;188:337–56. https://doi.org/10.1016/j.combustflame.2017.09.044.
[10] Boehm R, Yang Z, Bell DC, Feldhausen J, Heyne JS. Lower heating value of jet fuel from hydrocarbon class concentration data and thermo-chemical reference data: an uncertainty quantification. Fuel 2021. https://doi.org/10.1016/j.fuel.2021.1225.
[11] Dussan K, Won SH, Ure AD, Dryer FL, Dooley S. Chemical functional group descriptor for ignition propensity of large hydrocarbon liquid fuels. Proc Combust Inst 2019;37(4):5083–93. https://doi.org/10.1016/j.proci.2018.05.079.
[12] Wang Y, Wei W, Zhang Y, Hanson RK. A new strategy of characterizing hydrocarbon fuels using FTIR spectra and generalized linear model with grouped-Lasso regularization. Fuel 2021;287:119419. https://doi.org/10.1016/j.fuel.2020.119419.
[13] Wang Y, Ding Y, Wei W, Cao Y, Davidson DF, Hanson RK. On estimating physical and chemical properties of hydrocarbon fuels using mid-infrared FTIR spectra and regularized linear models. Fuel 2019;255:115715. https://doi.org/10.1016/j.fuel.2019.115715.
[14] Vozka P, Kilaz G. A review of aviation turbine fuel chemical composition-property relations. FUEL 2020;268. doi:10.1016/j.fuel.2020.117391.
[15] Shi X, Li H, Song Z, Zhang X, Liu G. Quantitative composition-property relationship of aviation hydrocarbon fuel based on comprehensive two-dimensional gas chromatography with mass spectrometry and flame ionization detector. Fuel 2017;200:395–406. https://doi.org/10.1016/j.fuel.2017.03.073.
[16] Abdul Jameel AG, Naser N, Issayev G, Touitou J, Ghosh MK, Emwas A-H, et al. A minimalist functional group (MFG) approach for surrogate fuel formulation. Combust Flame 2018;192:250–71. https://doi.org/10.1016/j.combustflame.2018.01.036.
[17] Pinkowski NH, Ding Y, Johnson SE, Wang Y, Parise TC, Davidson DF, et al. A multi-wavelength speciation framework for high-temperature hydrocarbon pyrolysis. J Quant Spectrosc Radiat Transf 2019;225:180–205. https://doi.org/10.1016/j.jqsrt.2018.12.038.
[18] Bell DC, Heyne JS, Won SH, Dryer FL. The impact of preferential vaporization on lean blowout in a referee combustor at figure of merit conditions. ASME Proc| Fuels, Combust Mater Handl 2018. https://doi.org/10.1115/POWER2018-7432.
[19] Striebich RC, Motsinger MA, Rauch ME, Zabarnick S, Dewitt M. Estimation of select specification tests for aviation turbine fuels using fast gas chromatography (GC). Energy Fuels 2005;19(6):2445–54. https://doi.org/10.1021/ef050136o.
[20] Trinklein TJ, Prebihalo SE, Warren CG, Ochoa GS, Synovec RE. Discovery-based analysis and quantification for comprehensive three-dimensional gas chromatography flame ionization detection data. J Chromatogr A 2020;1623:461190. https://doi.org/10.1016/j.chroma.2020.461190.
[21] Johnson KJ, Loegel TN, Metz AE, Wrzesinski PJ, Shafer LM, Striebich R, et al. Method for Detailed Hydrocarbon Analysis of Middle Distillate Fuels by Two-Dimensional Gas Chromatography. 2020.
[22] Wang F-Y. Comprehensive two-dimensional gas chromatography hyphenated with a vacuum ultraviolet spectrometer to analyze diesel-A three-dimensional separation (GC × GC × VUV) approach. Energy Fuels 2020;34(7):8012–7. https://doi.org/10.1021/acs.energyfuels.0c00688.
[23] Anthony IGM, Brantley MR, Gaw CA, Floyd AR, Solouki T. Vacuum ultraviolet spectroscopy and mass spectrometry: a tandem detection approach for improved identification of gas chromatography-eluting compounds. Anal Chem 2018;90(7):4878–85. https://doi.org/10.1021/acs.analchem.8b00531.
[24] Lelevic A, Souchon V, Moreaud M, Lorentz C, Geantet C. Gas chromatography vacuum ultraviolet spectroscopy: a review. J Sep Sci 2020;43(1):150–73. https://doi.org/10.1002/jssc.201900770.
[25] Lelevic A, Geantet C, Moreaud M, Lorentz C, Souchon V. Quantitative analysis of hydrocarbons in gas oils by two- dimensional comprehensive gas chromatography with vacuum ultraviolet detection. Energy Fuels 2021;35(17):13766–75. https://doi.org/10.1021/acs.energyfuels.1c01910.
[26] D02 Committee. ASTM D7566: Specification for Aviation Turbine Fuel Containing Synthesized Hydrocarbons. Conshokocken, PA: ASTM International; 2020. 10.1520/D7566-20.
[27] Dooley S, Won SH, Chaos M, Heyne J, Ju Y, Dryer FL, et al. A jet fuel surrogate formulated by real fuel properties. West States Sect Combust Inst Spring Tech Meet 2010;157(12):2333–9.
[28] Dooley S, Won SH, Heyne J, Farouk TI, Ju Y, Dryer FL, et al. The experimental evaluation of a methodology for surrogate fuel formulation to emulate gas phase combustion kinetic phenomena. Combust Flame 2012;159(4):1444–66. https://doi.org/10.1016/j.combustflame.2011.11.002.
[29] Yang Z, Stachler R, Heyne JS. Orthogonal reference surrogate fuels for operability testing. Energies 2020;13:1–13. https://doi.org/10.3390/en13081948.
[30] Kosir S, Stachler R, Heyne J, Hauck F. High-performance jet fuel optimization and uncertainty analysis. Fuel 2020;281:118718. https://doi.org/10.1016/j.fuel.2020.118718.
[31] Kosir S, Heyne J, Graham J. A machine learning framework for drop-in volume swell characteristics of sustainable aviation fuel. Fuel 2020;274:117832. https://doi.org/10.1016/j.fuel.2020.117832.
[32] Bell D, Heyne JS, August E, Won SH, Dryer FL, Haas FM, et al. On the development of general surrogate composition calculations for chemical and physical properties. AIAA SciTech Forum - 55th AIAA Aerosp Sci Meet 2017. https://doi.org/10.2514/6.2017-0609.
[33] Flora G, Kosir S, Heyne J, Zabarnik S, Gupta M. Properties calculator and optimization for drop-in alternative jet fuel blends. AIAA SciTech 2019:1–4.
[34] Boehm RC, Scholla LC, Heyne JS. Sustainable alternative fuel effects on energy consumption of jet engines. Fuel 2021;304:121378. https://doi.org/10.1016/j.fuel.2021.121378.
[35] Edwards T. Reference Jet Fuels for Combustion Testing. 55th AIAA Aerosp Sci Meet 2017:1–58. doi:10.2514/6.2017-0146.
[36] Colket M, Heyne J, Lieuwen TC, editors. Fuel Effects on Operability of Aircraft Gas Turbine Combustors. Reston, VA: American Institute of Aeronautics and Astronautics, Inc.; 2021.
[37] Peiffer EE, Heyne JS, Colket M. Sustainable aviation fuels approval streamlining: auxiliary power unit lean blowout testing. AIAA J 2019;57(11):4854–62. https://doi.org/10.2514/1.J058348.
[38] Boehm RC, Colborn JG, Heyne JS. Comparing alternative jet fuel dependencies between combustors of different size and mixing approaches. Front Energy Res 2021;9. https://doi.org/10.3389/fenrg.2021.701901.
[39] Stachler R, Heyne J, Stouffer S, Miller J. Lean blowoff in a toroidal jet-stirred reactor: implications for alternative fuel approval and potential mechanisms for autoignition and extinction. Energy Fuels 2020;34(5):6306–16. https://doi.org/10.1021/acs.energyfuels.9b01644.
[40] ASTM. Standard Specification for Aviation Turbine Fuel Containing Synthesized Hydrocarbons. Annu B ASTM Stand 2017:1–16. doi:10.1520/D1655-10.2.
[42] Colket MB, Heyne JS, Rumizen M, Edwards JT, Gupta M, Roquemore WM, et al. An overview of the national jet fuels combustion program. AIAA J 2017. https://doi.org/10.2514/6.2016-0177.

Technical Report Documentation Page

1. Report No.	2. Government Accession No.	3. Recipient's Catalog No.
j.fuel.2021.122709		

4. Title and Subtitle	5. Report Date
Towards fuel composition and properties from Two-dimensional gas chromatography with flame ionization and vacuum ultraviolet spectroscopy	December 2021
	6. Performing Organization Code

7. Author(s)	8. Performing Organization Report No.
Joshua Heyne, David Bell, John Feldhausen, Zhibin Yang, Randall Boehm	

9. Performing Organization Name and Address	10. Work Unit No. (TRAIS)
Center of Excellence for: Alternative Jet Fuels and Environment University of Dayton, Dayton, OH, USA	11. Contract or Grant No. 13-C-AJFF-UD-026

12. Sponsoring Agency Name and Address	13. Type of Report and Period Covered
Federal Aviation Administration Office of Environment and Energy	Journal Article
	14. Sponsoring Agency Code

15. Supplementary Notes

16. Abstract

Already low volume (<1mL) test methods facilitate the development of sustainable aviation fuel platforms and higher fidelity computational methods. Here a novel technique with two-dimensional gas chromatography (GCxGC) and Vacuum Ultraviolet (VUV) identification is used to characterize fuel composition and determine properties compared to previous work. Ten properties are predicted, including the temperature dependence of density, viscosity, thermal conductivity, and heat capacity. Property predictions incorporate uncertainty quantification (UQ) from analyte quantification (UQ1), root property uncertainty (UQ2), and the uncertainty associated with isomeric variance (UQ3), when an analyte is not identified via VUV. Comparisons to a previous method illustrate the ability of VUV identification to increase the fidelity of property predictions and decrease uncertainties. This method is applied to a surrogate intended to mimic the first-order properties and composition of a representative Jet A/A-1. In addition to nominal and temperature-dependent properties, the derived cetane number (DCN) of the surrogate is calculated for the distillation fraction evolved. The DCN there is shown to vary across the fraction of fuel distilled. Collectively, this method documents a process to prescreen novel sustainable aviation fuel candidates, facilitate the development of chemical process models, and automate property determinations for computational fluid dynamics.

17. Key Words	18. Distribution Statement
Property modeling, Jet fuel, Sustainable aviation fuel, GCxGC, VUV, ASCENT	

19. Security Classif. (of this report)	20. Security Classif. (of this page)	21. No. of Pages	22. Price
Unclassified	Unclassified		